

CNRS  
*Centre National de la Recherche Scientifique*

INFN  
*Istituto Nazionale di Fisica Nucleare*



## **Modal Interferometer Simulation**

VIR-0142A-10

Gabriele Vajente  
*INFN sezione di Pisa and Pisa University*

*Issue: 1*

*Date: February 22, 2010*

VIRGO \* A joint CNRS-INFN Project  
Via E. Amaldi, I-56021 S. Stefano a Macerata - Cascina (Pisa)  
Secretariat: Telephone (39) 050 752 521 \* FAX (39) 050 752 550 \* Email W3@virgo.infn.it

## Contents

<b>1</b>	<b>Introduction</b>	<b>1</b>
<b>2</b>	<b>Matrix operators for optical elements</b>	<b>2</b>
2.1	Mirror . . . . .	2
2.2	Tilted mirror . . . . .	3
2.3	Lens . . . . .	3
2.4	Free space propagation . . . . .	3
<b>3</b>	<b>Static fields</b>	<b>3</b>
3.1	Cavity resonant mode . . . . .	3
3.2	Fabry-Perot cavity . . . . .	4
3.2.1	Resonance condition . . . . .	5
3.3	Michelson interferometer . . . . .	6
3.3.1	Resonance conditions . . . . .	6
3.3.2	Input from anti-symmetric port . . . . .	7
3.4	Dual-recycled interferometer . . . . .	7
3.4.1	Power recycling resonance condition . . . . .	8
3.4.2	Input fields for arms . . . . .	8
3.4.3	Signal recycling resonance condition . . . . .	9
<b>4</b>	<b>Interferometer response to differential strain</b>	<b>9</b>
4.1	Fabry-Perot cavity response . . . . .	9
4.2	Michelson interferometer . . . . .	10
4.3	Dual-recycled interferometer response . . . . .	10
<b>5</b>	<b>Input mirror thermal lensing</b>	<b>12</b>
<b>6</b>	<b>Summary of all relevant equations</b>	<b>13</b>
<b>7</b>	<b>List of symbols</b>	<b>15</b>

## 1 Introduction

This document describes a modal simulation of dual-recycled interferometers. Equations are given to compute the steady state fields (carrier, radio-frequency and audio sidebands) inside a general interferometer, as well as the detector response to differential strain. All fields are described in terms of a development in Hermite-Gauss modes in the basis of the arm Fabry-Perot cavities. In this framework all mirrors and optical elements are described by matrix operators that couple different modes if the element are not well matched to the beam. This analysis is similar to the one presented in [1] and [2].

At each point inside the interferometer the fields can be expressed as vectors of complex coefficient in a given Gaussian basis. In this computation the unperturbed arm basis is always used: the two arms are taken as equal and their mode computed. This mode is used as the basis one for all fields, even outside the long arm cavities. In this approach the only approximation is to neglect the influence of the Schnupp asymmetry for the Gaussian basis.

The steady state equations for the fields inside a dual recycled interferometer are written in vector notation and analytically solved. Once the operator matrices for each optical element are known, the result can be numerically computed.

## 2 Matrix operators for optical elements

### 2.1 Mirror

If the mirror is perfectly matched to the incoming Gaussian beam its surface corresponds to the wave-front of the field and the reflection as well as the transmission are unity operators, since no modification is done to the beam.

If the mirror is instead not matched, its shape can be expressed as the deviation from the constant phase surface of the Gaussian beam  $z(x, y)$  which is taken as a general function of the two transverse variables  $x$  and  $y$ .

If the incoming beam at the mirror is  $\psi_{in}(x, y)$ , the reflected one acquires a phase shift dependent on transverse variables  $x$  and  $y$

$$\psi_{ref}(x, y) = e^{2ikZ(x,y)}\psi_{in}(x, y) \quad (2.1)$$

begin  $k$  the incoming beam wave vector  $k = 2\pi/\lambda$ .

The mirror operator is a matrix in the Gauss-Hermite basis. The element give the coupling coefficient of a  $TEM_{n,m}$  mode into a reflected  $TEM_{p,q}$ . This can be obtained numerically from the scalar product

$$M_{pq,nm} = \left\langle U_{pq}, e^{2ikZ(x,y)}\psi_{in}(x, y)U_{mn} \right\rangle \quad (2.2)$$

For reference the explicit expression of a  $n, m$  Gauss-Hermite mode is reported here [3]:

$$U_{mn} = \sqrt{\frac{2}{\pi}} \sqrt{\frac{1}{2^{n+m} m! n! w^2(z)}} H_m \left( \frac{\sqrt{2}}{w(z)} x \right) H_n \left( \frac{\sqrt{2}}{w(z)} y \right) \exp \left[ -(x^2 + y^2) \left( \frac{1}{w^2(z)} + \frac{ik}{2R(z)} \right) \right] \quad (2.3)$$

$$w(z) = w_0 \sqrt{1 + \left( \frac{z}{z_0} \right)^2} \quad (2.4)$$

$$R(z) = z + \frac{z_0^2}{z} \quad (2.5)$$

$$z_0 = \frac{\pi w_0^2}{\lambda} \quad (2.6)$$

In this expression the Gouy phase is not written in the fundamental modes, since it is considered inside the propagators. Here  $H_m$  is the Hermite polynomial of order  $n$ .

Using the same Gauss-Hermite basis for the incoming and reflected beam, the matrix operator for a general mirror is given by the following integral:

$$M_{pq,mn} = \frac{2}{\pi w^2(z)} \sqrt{\frac{1}{2^{m+n+p+q} m! n! p! q!}} \int_{-\infty}^{+\infty} \int_{-\infty}^{+\infty} H_p \left( \frac{\sqrt{2}}{w(z)} x \right) H_q \left( \frac{\sqrt{2}}{w(z)} y \right) H_m \left( \frac{\sqrt{2}}{w(z)} x \right) H_n \left( \frac{\sqrt{2}}{w(z)} y \right) e^{2ikZ(x,y)} e^{-\frac{2(x^2+y^2)}{w^2(z)}} dx dy \quad (2.7)$$

Once the profile of the mirror surface is known, this matrix can be computed by simple numerical integration. In the simple case of a spherical mismatched mirror, the surface deviation is given by

$$Z(z, y) = \frac{x^2 + y^2}{2} \left( \frac{1}{R_C} - \frac{1}{R(z)} \right) \quad (2.8)$$

where  $R_C$  is the mirror radius of curvature and  $R(z)$  is the beam phase front curvature at the mirror.

In the actual model mirrors are considered as thin objects, without any substrate. Therefore there is no effect of a mismatched mirror in transmission. This can be easily implemented in future if needed.

The reflection matrix from the other side of the mirror is simply given by the inverse of the computed operator. Being the reflection matrices unitary, it is enough to take the hermitian transpose.

## 2.2 Tilted mirror

If the tilt angle is small, at first order the beam dephasing can be expressed as [4]:

$$Z(z, y) = \frac{x^2 + y^2}{2} \left( \frac{1}{R_C} - \frac{1}{R(z)} \right) + \theta x \quad (2.9)$$

where  $\theta$  is the tilt angle measured in radians.

## 2.3 Lens

The effect of transmission through a thin lens with a given focal length  $f$  can be described again as the addition of a dephasing, given this time by [3]:

$$\psi_{tra}(x, y) = \psi_{in}(x, y) e^{ik \frac{x^2 + y^2}{2f}} \quad (2.10)$$

and the lens operator can be computed with the same equations as for mismatched mirrors. It is interesting to see that the lens matrix depends only on the focal length and on the beam spot size at the lens.

## 2.4 Free space propagation

The propagation through free space is a diagonal operator which takes into account the Gouy phase accumulated by the different Hermite-Gauss modes:

$$\phi_g = \arctan \left( \frac{z}{z_0} \right) \quad (2.11)$$

where  $z$  is the distance of the point considered with respect to the beam waist. The phase in propagation through a given length is computed as the difference between the Gouy phase at the two extremes.

The propagation matrix is given by

$$P_{mn} = \exp \left( ikL + i \frac{\omega}{c} L + (m + n) \psi_g \right) \quad (2.12)$$

In this equation the carrier field is considered to have null frequency. The propagator for audio or radio-frequency sidebands can be obtained by setting the  $\omega$  variable. The Gouy phase of the fundamental  $TEM_{00}$  mode is not considered, since it is in any case canceled by a proper setting of the resonance condition.

# 3 Static fields

## 3.1 Cavity resonant mode

The simulation Hermite-Gauss basis is fixed by the Fabry-Perot arm cavity: its length is  $L$  and the radii of curvature of the two mirrors are  $L_1$  (input) and  $L_2$  (end). The relevant parameters of the resonant mode are

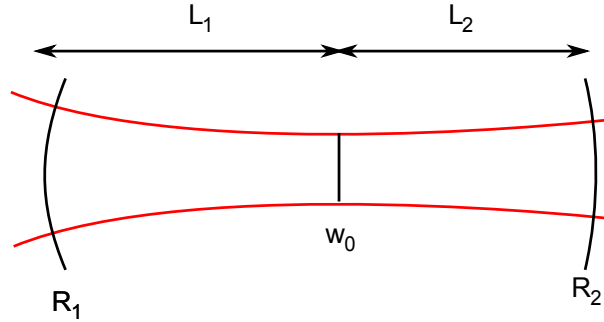


Figure 1: Scheme of a single resonant Fabry-Perot cavity.  $R_1$  and  $R_2$  are the two radii of curvature.  $L_1$  and  $L_2$  the distance of the two mirrors from the cavity mode waist. The cavity length is  $L$ .

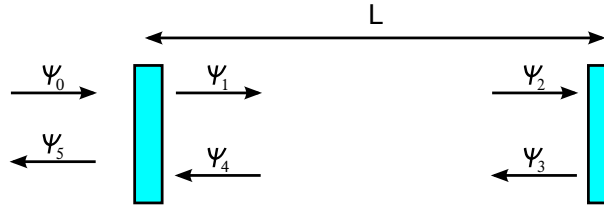


Figure 2: Fields for the computations of Fabry-Perot cavity operators.

the position of the waist and the Rayleigh range. The distance of the waist from the input mirrors are given by

$$L_1 = \frac{L(R_2 - L)}{R_1 + R_2 - 2L} \quad (3.1)$$

$$L_2 = \frac{L(R_1 - L)}{R_1 + R_2 - 2L} \quad (3.2)$$

and the Rayleigh length is:

$$z_0^2 = \frac{(R_1 - L)(R_2 - L)(R_1 + R_2 - L)L}{(R_1 + R_2 - 2L)^2} \quad (3.3)$$

### 3.2 Fabry-Perot cavity

A single Fabry-Perot cavity is composed by an input mirror and an end mirror, with scalar amplitude reflection coefficients  $r_i$  and  $r_e$  and scalar amplitude transmission coefficients  $t_i$  and  $t_e$ . Here the convention of [4] is used for mirror reflection and transmission. If we consider the more general case of mismatched mirrors, the reflection and transmission coefficients are matrix, as described in sec. 2.1. These matrices are supposed to contain also the scalar coefficients for the mirror.

The field inside the cavity obeys the following steady state equation (see fig. 2):

$$\psi_1 = T_i \psi_0 - R_i P_L R_e P_L \psi_1 \quad (3.4)$$

where  $R_i$  and  $R_e$  are the reflection operators for input and end mirrors,  $P_L$  is the propagator for the cavity length  $L$ , taking into account also the Gouy phase as explained in sec. 2.4. One must take care that all these equations contains matrix operand, therefore ordering matters. The intra-cavity field can be obtained solving eq. 3.4:

$$\psi_1 = (1 + R_i P_L R_e P_L)^{-1} T_i \psi_0 \quad (3.5)$$

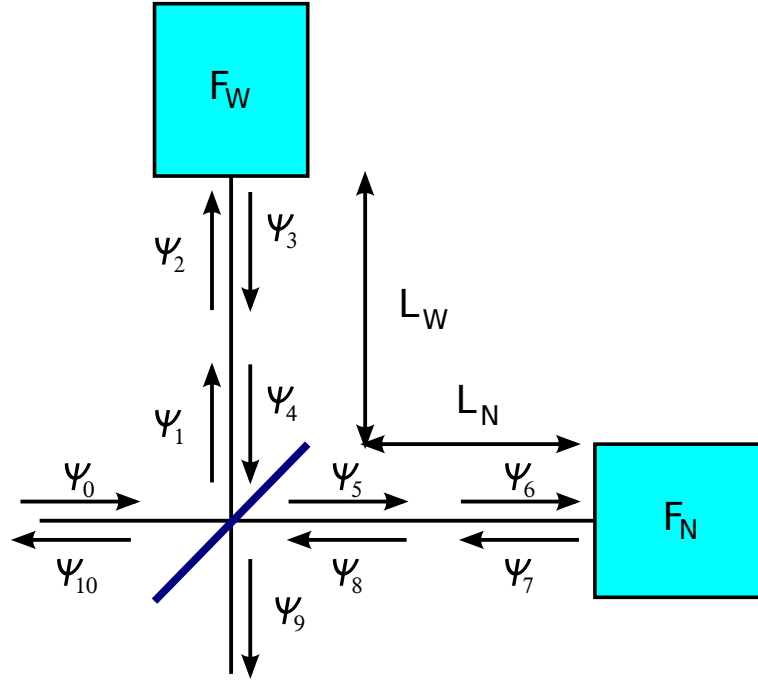


Figure 3: Fields for the computations of Michelson interferometer operators.

To build more complex interferometers we need an analytical expression for the reflected field and for the field impinging on the end mirror:

$$F = i \left[ R_i^+ + T_i P_L R_e P_L (1 + R_i P_L R_e P_L)^{-1} T_i \right] \quad (\text{reflection operator}) \quad (3.6)$$

$$I = P_L (1 + R_i P_L R_e P_L)^{-1} T_i \quad (\text{intra-cavity field operator}) \quad (3.7)$$

### 3.2.1 Resonance condition

It is useful to specify the propagator expression in order to express the cavity length tuning as an offset from resonance of the fundamental  $TEM_{00}$  mode. In the approximation of well matched mirrors and considering only the fundamental mode, the intra-cavity field is given by

$$\psi_1 = \frac{t_i}{1 + r_i r_e e^{2ikL}} \psi_0$$

At resonance the exponential must be equal to  $-1$  and therefore the propagator for a Fabry-Perot cavity around resonance can be written as

$$(P_L)_{mn,pq} = i e^{ik\delta L + i(m+n)\phi_g} \delta_{mp} \delta_{nq} \quad (3.8)$$

### 3.3 Michelson interferometer

Referring to fig. 3, with an input from the symmetric port, the fields inside a general Michelson interferometer must satisfy the steady state equations:

$$\begin{aligned}\psi_4 &= P_W F_W P_W \frac{i}{\sqrt{2}} \psi_0 \\ \psi_8 &= P_N F_N P_N \frac{1}{\sqrt{2}} \psi_0 \\ \psi_9 &= \frac{1}{\sqrt{2}} \psi_4 + \frac{i}{\sqrt{2}} \psi_8 \\ \psi_{10} &= \frac{i}{\sqrt{2}} \psi_4 + \frac{1}{\sqrt{2}} \psi_8\end{aligned}$$

where  $F_N$  and  $F_W$  are the generic reflection operators of the two arms. Here the beam-splitter is assumed to be perfect. These equations can be solved for the symmetric and anti-symmetric port fields:

$$\psi_9 = \frac{i}{2} (P_N F_N P_N + P_W F_W P_W) \psi_0 \quad (3.9)$$

$$\psi_{10} = \frac{1}{2} (P_N F_N P_N - P_W F_W P_W) \psi_0 \quad (3.10)$$

At this point it is very useful to define the common and differential Michelson propagators

$$P_+ = P_{N/2} P_{W/2} \quad (3.11)$$

$$P_- = P_{N/2} P_{-W/2} \quad (3.12)$$

Since propagators are diagonal and thus commutant, the following identities hold:

$$P_N = P_+ P_- \quad (3.13)$$

$$P_W = P_+ P_-^{-1} \quad (3.14)$$

Equations 3.9 and 3.10 can be rewritten in terms of the Michelson transmission operators from symmetric port to symmetric and anti-symmetric ports:

$$M_{SA} = \frac{i}{2} P_+ (P_- F_N P_- + P_-^{-1} F_W P_-^{-1}) P_+ \quad (3.15)$$

$$M_{SS} = \frac{1}{2} P_+ (P_- F_N P_- - P_-^{-1} F_W P_-^{-1}) P_+ \quad (3.16)$$

#### 3.3.1 Resonance conditions

As for the Fabry-Perot, it is useful to enforce in the propagators the dark fringe condition in the case of Fabry-Perot arms. If the arms are at resonance, their reflection coefficients can be well approximated with  $F_N \sim F_W \sim -i$ . The dark fringe field is therefore

$$\psi_9 \sim \frac{1}{2} e^{2ikl_+} (e^{2ikl_-} + e^{-2ikl_-}) e^{2ikl_+}$$

This field should be zero and this enforce the condition  $e^{2ikl_-} = i$  from which the final expression for the Michelson differential propagator around dark fringe can be found:

$$(P_-)_{pq, mn} = \sqrt{i} e^{ik\delta l_-} \delta_{mp} \delta_{nq} \quad (3.17)$$

Note that here the Gouy phase in propagation through the macroscopic Michelson differential length (Schnupp asymmetry) is neglected.

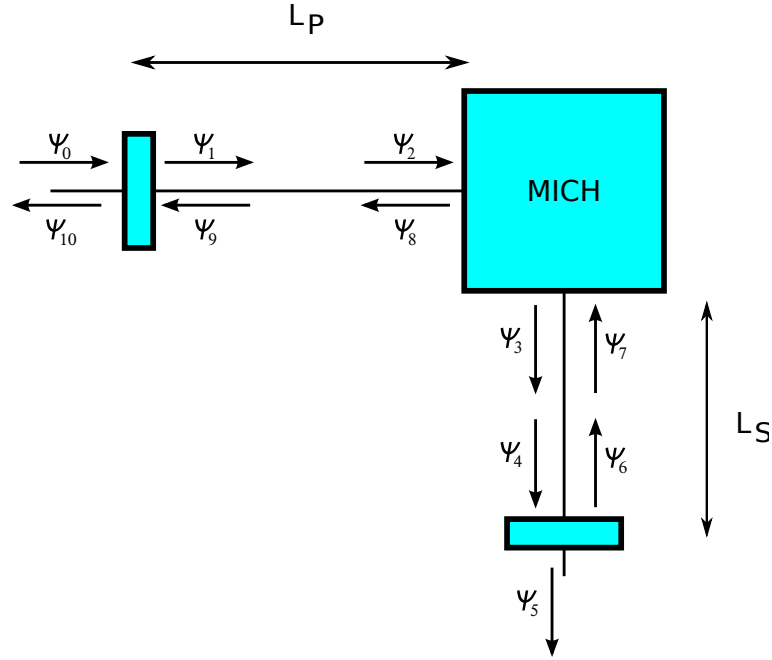


Figure 4: Scheme of fields inside a dual recycled interferometer.

### 3.3.2 Input from anti-symmetric port

To implement signal recycling, one also needs the Michelson equation for an input from the anti-symmetric port. From a simple symmetry argument it appears that they can be obtained from the above equation, just swapping north and west. In conclusion one can find that:

$$M_{AS} = M_{SA} \quad (3.18)$$

$$M_{AA} = -M_{SS} \quad (3.19)$$

## 3.4 Dual-recycled interferometer

Static field equations for a dual recycled interferometer can be obtained considering the Michelson part as a box with the already computed transmittance operators. Referring to fig. 4 the fields  $\psi_1$  and  $\psi_4$  inside the two recycling cavities are used as basic fields:

$$\begin{aligned} \psi_1 &= T_P \psi_0 + iR_P P_P M_{SS} P_P \psi_1 - R_P P_P M_{AS} P_S R_S \psi_4 \\ \psi_4 &= P_S M_{SA} P_P \psi_1 + iP_S M_{AA} P_S R_S \psi_4 \end{aligned}$$

One can solve for  $\psi_4$  from the second equation obtaining:

$$\psi_4 = (1 - iP_S M_{AA} P_S R_S)^{-1} P_S M_{SA} P_P \psi_1$$

and substitute in the first one to get a final expression for the power recycling cavity field:

$$\psi_1 = \left[ 1 - iR_P P_P M_{SS} P_P + R_P P_P M_{AS} P_S R_S (1 - iP_S M_{AA} P_S R_S)^{-1} P_S M_{SA} P_P \right]^{-1} T_P \psi_0 \quad (3.20)$$

### 3.4.1 Power recycling resonance condition

To set the correct operating point around the power recycling resonance one assumes there is no signal recycling  $R_S = 0$  and approximate to the case of only fundamental  $TEM_{00}$  mode and no mismatching:

$$\psi_1 = \frac{t_p}{1 - ir_p(P_P P_+)^2} \quad (3.21)$$

The power recycling cavity propagator can be defined as

$$P_{RC} = P_+ P_P \quad (3.22)$$

and considering displacement from the carrier fundamental mode resonance it is equal to

$$(P_{RC})_{pq,mn} = \sqrt{-1} e^{ik\delta l_{RC} + i(m+n)\phi_{g,RC}} \delta_{mp} \delta_{nq} \quad (3.23)$$

where  $\phi_{g,RC}$  is the Gouy phase in propagation inside the recycling cavity.

It is useful to rewrite eq. 3.20 in terms of this new power recycling propagator and the equivalent signal recycling propagator:

$$P_{SC} = P_S P_+ \quad (3.24)$$

For this purpose, a redefinition of the Michelson operators, factorizing out the  $P_+$  is useful:

$$\begin{aligned} P_P M_{SS} P_P &= P_{RC} M'_{SS} P_{RC} \\ P_P M_{AS} P_S &= P_{RC} M'_{AS} P_{SC} \\ P_S M_{SA} P_P &= P_{SC} M'_{SA} P_{RC} \\ P_S M_{AA} P_S &= P_{SC} M'_{AA} P_{SC} \end{aligned}$$

where

$$\begin{aligned} M'_{SS} &= \frac{1}{2} (P_- F_N P_- - P_-^{-1} F_W P_-^{-1}) \\ M'_{AS} &= \frac{i}{2} (P_- F_N P_- + P_-^{-1} F_W P_-^{-1}) \end{aligned}$$

and similar for  $M'_{AA}$  and  $M'_{SA}$ . With these new definitions, the field inside power recycling cavity is given by:

$$\psi_1 = \left[ 1 - iR_P P_{RC} M'_{SS} P_{RC} + R_P P_{RC} M'_{AS} P_{SC} R_S (1 - iP_{SC} M'_{AA} P_{SC} R_S)^{-1} P_{SC} M'_{SA} P_{RC} \right]^{-1} T_P \psi_0 \quad (3.25)$$

The field inside the signal recycling cavity is:

$$\psi_4 = (1 - iP_{SC} M'_{AA} P_{SC} R_S)^{-1} P_{SC} M'_{SA} P_{RC} \psi_1 \quad (3.26)$$

### 3.4.2 Input fields for arms

To compute the fields inside the two Fabry-Perot arm cavities, we first need the Michelson input fields  $\psi_2$  and  $\psi_7$ :

$$\begin{aligned} \psi_2 &= P_P \psi_1 \\ \psi_4 &= iP_S R_S \psi_4 \end{aligned}$$

and using equations from the Michelson interferometer (see sec. 3.3) we can compute the fields in input of the two Fabry-Perot arms:

$$\begin{aligned} \psi_N &= \frac{1}{\sqrt{2}} P_N \psi_2 + \frac{i}{\sqrt{2}} P_N \psi_7 \\ \psi_W &= \frac{i}{\sqrt{2}} P_W \psi_2 + \frac{1}{\sqrt{2}} P_W \psi_7 \end{aligned}$$

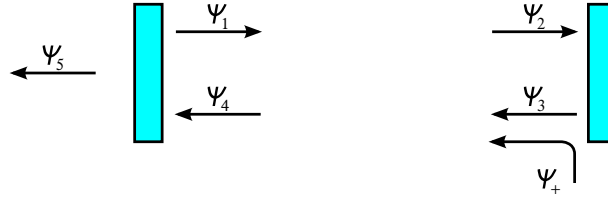


Figure 5: Fields for the computations of Fabry-Perot cavity response to end mirror motion.

These can be rewritten in terms of the power recycling cavity fields  $\psi_1$ :

$$\psi_N = \frac{1}{\sqrt{2}} \left[ P_- P_{RC} - P_- P_{SC} R_S (1 - iP_{SC} M'_{AA} P_{SC} R_S)^{-1} P_{SC} M'_{SA} P_{RC} \right] \psi_1 \quad (3.27)$$

$$\psi_W = \frac{i}{\sqrt{2}} \left[ P_-^{-1} P_{RC} - P_-^{-1} P_{SC} R_S (1 - iP_{SC} M'_{AA} P_{SC} R_S)^{-1} P_{SC} M'_{SA} P_{RC} \right] \psi_1 \quad (3.28)$$

Then the intra-cavity fields can be computed using eq. 3.7.

### 3.4.3 Signal recycling resonance condition

To get the correct resonance condition inside the signal recycling one must start again from the well-matched fundamental mode approximation. The field inside SRC is given by eq. 3.26 and its resonance depends on the  $M'_{AA}$  operator. With arms on resonance and close to dark fringe it is well approximated by  $M'_{AA} \sim -1$ . Defining  $\psi_{pump} = P_{SC} M'_{SA} P_{RC} \psi_1$ , eq. 3.26 is approximated by

$$\psi_4 \sim \frac{\psi_{pump}}{1 + ie^{2ikl_{SC}} r_s}$$

Here we assume zero tuning of signal recycling when the carrier field is anti-resonant and therefore

$$(P_{SC})_{pq,mn} = \sqrt{-i} e^{i\varphi_{SRC} + i(m+n)\varphi_{g,SC}} \delta_{pm} \delta_{nq} \quad (3.29)$$

where the signal recycling tuning  $\varphi_{SRC}$  has been introduced.

## 4 Interferometer response to differential strain

### 4.1 Fabry-Perot cavity response

To compute the dark port signal response to a differential motion of the end mirror one must start from the expression of the Fabry-Perot cavity response to an end mirror motion at a given frequency. The effect can be described as an additional input to the cavity fields at the end mirror reflection port which contains a dephasing modulated at the frequency of the motion (see fig. 5). Using the same notations introduced in sec. 3.2:

$$\psi_R = ir_e e^{2ikx(t)} \psi_2 \sim ir_e \psi_2 + ir_e \cdot 2ikx(t) \psi_2 \quad (4.1)$$

The additional field (at a frequency  $\omega$ ) is then given by

$$\psi_+(\omega) = -2kx_0 R_e \psi_2 \quad (4.2)$$

where  $x_0$  is the end mirror motion amplitude at the  $\omega$  frequency. This additional signal must then be propagated to the reflection port of the cavity:

$$\psi_3(\omega) = (1 + R_e P_L(\omega) R_i P_L(\omega))^{-1} \psi_+(\omega) \quad (4.3)$$

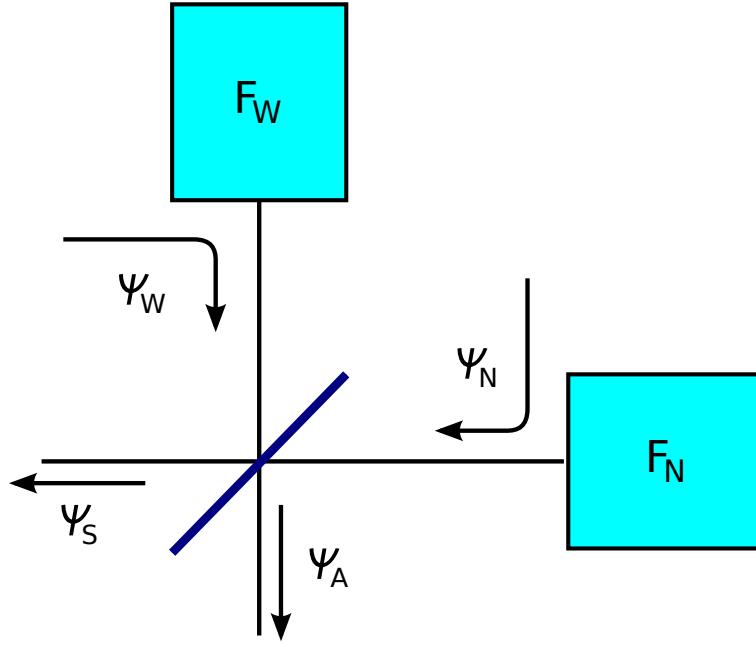


Figure 6: Signal sideband propagations inside Michelson interferometer.

where the propagator must take into account the signal frequency

$$P_L(\omega) = P_L e^{i\frac{\omega}{c}L} \quad (4.4)$$

In conclusion the field in reflection of the cavity at the signal frequency is given by

$$\psi_5(\omega) = -2kx_0 T_i P_L(\omega) (1 + R_e P_L(\omega) R_i P_L(\omega))^{-1} R_e \psi_2 \quad (4.5)$$

The second ingredient needed to build more complex systems is the cavity reflection operator at the signal frequency. This is the same as eq. 3.6 but computed at the signal frequency

$$F(\omega) = i \left[ R_i^+ + T_i P_L(\omega) R_e P_L(\omega) (1 + R_i P_L(\omega) R_e P_L(\omega))^{-1} T_i \right] \quad (4.6)$$

## 4.2 Michelson interferometer

In the case of differential motion inside the arms, two fields are added inside the Michelson interferometer at the two arm reflection ports. They propagate both to the symmetric and anti-symmetric port (see fig. 6):

$$\psi_A(\omega) = \frac{1}{\sqrt{2}} P_+(\omega) (i P_-(\omega) \psi_N(\omega) + P_-^{-1}(\omega) \psi_W(\omega)) \quad (4.7)$$

$$\psi_S(\omega) = \frac{1}{\sqrt{2}} P_+(\omega) (P_-(\omega) \psi_N(\omega) + i P_-^{-1}(\omega) \psi_W(\omega)) \quad (4.8)$$

Also the Michelson transmission coefficients are needed. They can be obtained from eq. 3.15, 3.16, 3.18, 3.19 just replacing the propagators with ones computed at the frequency  $\omega$ .

## 4.3 Dual-recycled interferometer response

Referring to fig. 7, signal sidebands coming from the arms can be seen as additional inputs at the level of the power and signal recycling cavities. We divide these inputs in the symmetric part (going inside PRC) and the

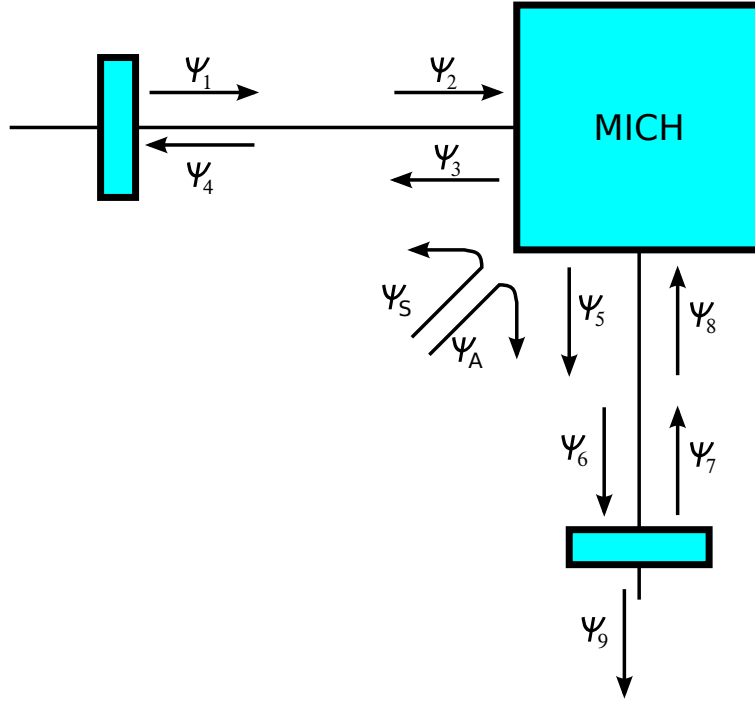


Figure 7: Signal sideband propagations inside a dual recycled interferometer.

anti-symmetric part (going inside SRC). The two fields  $\psi_3$  and  $\psi_5$  are considered as the basis one for the steady state equation. We need only  $\psi_5$  since we need to compute only the dark fringe response to differential motion.

$$\begin{aligned}\psi_3 &= \psi_S + iM_{SS}(\omega)P_P(\omega)R_P P_P(\omega)\psi_3 + iM_{AS}(\omega)P_S(\omega)R_S P_S(\omega)\psi_5 \\ \psi_5 &= \psi_A + iM_{SA}(\omega)P_P(\omega)R_P P_P(\omega)\psi_3 + iM_{AA}(\omega)P_S(\omega)R_S P_S(\omega)\psi_5\end{aligned}$$

The first equation can be solved to get  $\psi_3$

$$\psi_3 = (1 - iM_{SS}(\omega)P_P(\omega)R_P P_P(\omega))^{-1}\psi_S + i(1 - iM_{SS}(\omega)P_P(\omega)R_P P_P(\omega))^{-1}M_{AS}(\omega)P_S(\omega)R_S P_S(\omega)\psi_5$$

This is then substituted inside the second equation above to solve for  $\psi_5$ :

$$\begin{aligned}\psi_5 &= \left[ 1 - iM_{AA}(\omega)P_S(\omega)R_S P_S(\omega) + iM_{SA}(\omega)P_P(\omega)R_P P_P(\omega) \right. \\ &\quad \left. (1 - iM_{SS}(\omega)P_P(\omega)R_P P_P(\omega))^{-1}M_{AS}(\omega)P_S(\omega)R_S P_S(\omega) \right]^{-1} \\ &\quad \left[ \psi_A + iM_{SA}(\omega)P_P(\omega)R_P P_P(\omega)(1 - iM_{SS}(\omega)P_P(\omega)R_P P_P(\omega))^{-1}\psi_S \right]\end{aligned}\quad (4.9)$$

This equation must be rewritten to contain only physical propagators  $P_-$ ,  $P_{RC}$  and  $P_{SC}$ . The first step is to introduce again the modified Michelson operators defined in sec. 3.4.1. The partial propagators can be written as  $P_P = P_{RC}P_+^{-1}$  and  $P_S = P_{SC}P_+^{-1}$ . Using these equations, the commutation property of all propagator and the inverse of product identity  $(AB)^{-1} = B^{-1}A^{-1}$  one can reshuffle the previous equation only in term of the physical propagators:

$$\begin{aligned}\psi_{DF}(\omega) &= T_S P_{SC}(\omega) \left[ 1 - iM'_{AA}(\omega)P_{SC}(\omega)R_S P_{SC}(\omega) + iM'_{SA}(\omega)P_{RC}(\omega)R_P P_{RC}(\omega) \right. \\ &\quad \left. (1 - iM'_{SS}(\omega)P_{RC}(\omega)R_P P_{RC}(\omega))^{-1}M'_{AS}(\omega)P_{SC}(\omega)R_P P_{SC}(\omega) \right]^{-1} \\ &\quad \left[ \psi_A(\omega) + iM'_{SA}(\omega)P_{RC}(\omega)R_P P_{RC}(\omega)(1 - iM'_{SS}(\omega)P_{RC}(\omega)R_P P_{RC}(\omega))^{-1}\psi_S(\omega) \right]\end{aligned}\quad (4.10)$$

where the symmetric and anti-symmetric fields are

$$\begin{aligned}\psi_A(\omega) &= \frac{1}{\sqrt{2}} (iP_- \psi_N(\omega) + P_-^{-1} \psi_W(\omega)) \\ \psi_S(\omega) &= \frac{1}{\sqrt{2}} (P_- \psi_N(\omega) + iP_-^{-1} \psi_W(\omega))\end{aligned}$$

## 5 Input mirror thermal lensing

Thermal lensing in the input mirror substrate can be easily modeled with the small addition of a lens operator  $\Lambda$  at the input and output of the Fabry-Perot cavity operator. Therefore eq. 3.6 becomes

$$F = i\Lambda \left[ R_i^+ + T_i P_L R_e P_L (1 + R_i P_L R_e P_L)^{-1} T_i \right] \Lambda \quad (5.1)$$

The fields inside the two Fabry-Perot cavities (see sec. 3.4.2) become explicitly

$$\begin{aligned}\psi_N^{ins} &= \frac{1}{\sqrt{2}} P_{LN} (1 + R_{iN} P_{LN} R_{eN} P_{LN})^{-1} T_{iN} \Lambda_N \\ &\quad \left[ P_- P_{RC} - P_- P_{SC} R_S (1 - iP_{SC} M'_{AA} P_{SC} R_S)^{-1} P_{SC} M'_{SA} P_{RC} \right] \psi_{RC}\end{aligned} \quad (5.2)$$

$$\begin{aligned}\psi_W^{ins} &= \frac{1}{\sqrt{2}} P_{LW} (1 + R_{iW} P_{LW} R_{eW} P_{LW})^{-1} T_{iW} \Lambda_W \\ &\quad \left[ P_-^{-1} P_{RC} - P_-^{-1} P_{SC} R_S (1 - iP_{SC} M'_{AA} P_{SC} R_S)^{-1} P_{SC} M'_{SA} P_{RC} \right] \psi_{RC}\end{aligned} \quad (5.3)$$

Finally, the signal fields at the two cavity outputs are given by

$$\psi_N(\omega) = -2kx_N(\omega) \Lambda_N T_{iN} P_{LN}(\omega) (1 + R_{eN} P_{LN}(\omega) R_{iN} P_{LN}(\omega))^{-1} R_{eN} \psi_N^{ins} \quad (5.4)$$

$$\psi_W(\omega) = -2kx_W(\omega) \Lambda_W T_{iW} P_{LW}(\omega) (1 + R_{eW} P_{LW}(\omega) R_{iW} P_{LW}(\omega))^{-1} R_{eW} \psi_W^{ins} \quad (5.5)$$

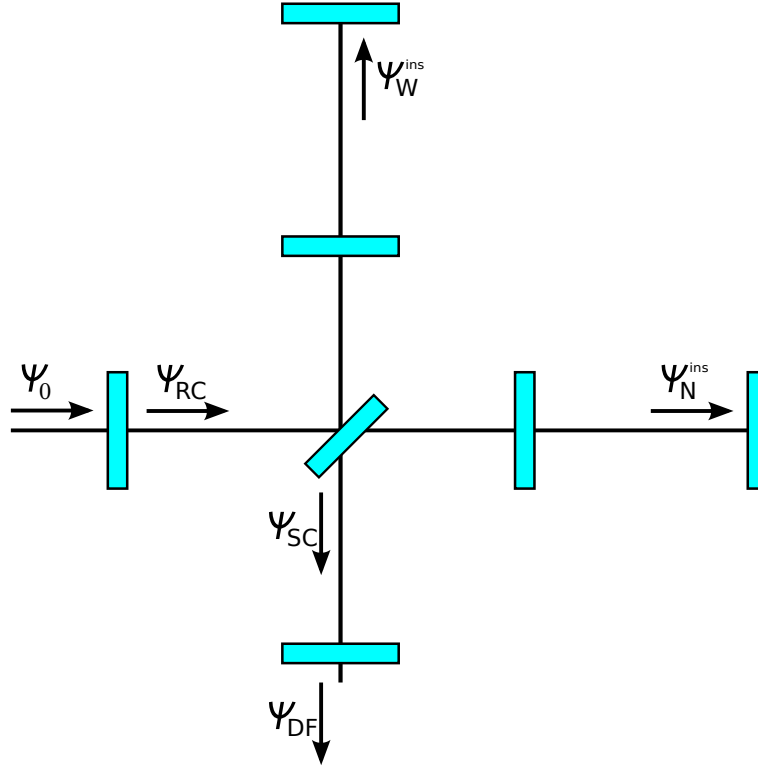


Figure 8: Relevant fields inside a dual-recycled Fabry-Perot interferometer.

## 6 Summary of all relevant equations

Fig. 8 shows the relevant fields computed in this analysis. This section summarizes all the equations computed in this note. Static fields are given by

$$\psi_{RC} = \left[ 1 - iR_P P_{RC} M'_{SS} P_{RC} + R_P P_{RC} M'_{AS} P_{SC} R_S (1 - iP_{SC} M'_{AA} P_{SC} R_S)^{-1} P_{SC} M'_{SA} P_{RC} \right]^{-1} T_P \psi_0$$

$$\psi_{SC} = (1 - iP_{SC} M'_{AA} P_{SC} R_S)^{-1} P_{SC} M'_{SA} P_{RC} \psi_{RC}$$

$$\psi_{DF} = T_S \psi_{SC}$$

$$M'_{SS} = -M'_{AA} = \frac{1}{2} (P_- F_N P_- - P_-^{-1} F_W P_-^{-1})$$

$$M'_{AS} = M'_{SA} = \frac{i}{2} (P_- F_N P_- + P_-^{-1} F_W P_-^{-1})$$

$$F_X = i\Lambda_X \left[ R_{iX}^+ + T_{iX} P_{LX} R_{eX} P_{LX} (1 + R_{iX} P_{LX} R_{eX} P_{LX})^{-1} T_{iX} \right] \Lambda_X$$

$$\psi_N^{ins} = \frac{1}{\sqrt{2}} P_{LN} (1 + R_{iN} P_{LN} R_{eN} P_{LN})^{-1} T_{iN} \Lambda_N \left[ P_- P_{RC} - P_- P_{SC} R_S (1 - iP_{SC} M'_{AA} P_{SC} R_S)^{-1} P_{SC} M'_{SA} P_{RC} \right] \psi_{RC}$$

$$\psi_W^{ins} = \frac{1}{\sqrt{2}} P_{LW} (1 + R_{iW} P_{LW} R_{eW} P_{LW})^{-1} T_{iW} \Lambda_W \left[ P_-^{-1} P_{RC} - P_-^{-1} P_{SC} R_S (1 - iP_{SC} M'_{AA} P_{SC} R_S)^{-1} P_{SC} M'_{SA} P_{RC} \right] \psi_{RC}$$

Around the standard working point the propagators are

$$\begin{aligned}
 (P_{LX})_{pq,mn} &= ie^{ik\delta L_X + i(n+m)\phi_{g,x}} \delta_{pm} \delta_{qn} \\
 (P_-)_{pq,mn} &= \sqrt{i} e^{ik\delta l_-} \delta_{pm} \delta_{qn} \\
 (P_{RC})_{pq,mn} &= \sqrt{-i} e^{ik\delta l_{RC} + i(n+m)\phi_{g,RC}} \delta_{pm} \delta_{qn} \\
 (P_{SC})_{pq,mn} &= \sqrt{-i} e^{i\varphi_{SC} + i(n+m)\phi_{g,RC}} \delta_{pm} \delta_{qn}
 \end{aligned}$$

Dark fringe response to end mirror motions is given by

$$\begin{aligned}
 \psi_{DF}(\omega) &= T_S P_{SC}(\omega) \left[ 1 - iM'_{AA}(\omega) P_{SC}(\omega) R_S P_{SC}(\omega) + iM'_{SA}(\omega) P_{RC}(\omega) R_P P_{RC}(\omega) \cdot \right. \\
 &\quad \left. (1 - iM'_{SS}(\omega) P_{RC}(\omega) R_P P_{RC}(\omega))^{-1} M'_{AS}(\omega) P_{SC}(\omega) R_P P_{SC}(\omega) \right]^{-1} \cdot \\
 &\quad \left[ \psi_A(\omega) + iM'_{SA}(\omega) P_{RC}(\omega) R_P P_{RC}(\omega) (1 - iM'_{SS}(\omega) P_{RC}(\omega) R_P P_{RC}(\omega))^{-1} \psi_S(\omega) \right] \\
 \psi_A(\omega) &= \frac{1}{\sqrt{2}} [iP_-(\omega)\psi_N(\omega) + P_-(\omega)^{-1}\psi_W(\omega)] \\
 \psi_S(\omega) &= \frac{1}{\sqrt{2}} [P_-(\omega)\psi_N(\omega) + iP_-(\omega)^{-1}\psi_W(\omega)] \\
 \psi_N(\omega) &= -2kx_N(\omega)\Lambda_N T_{iN} P_{LN}(\omega) (1 + R_{eN} P_{LN}(\omega) R_{iN} P_{LN}(\omega))^{-1} R_{eN} \psi_N^{ins} \\
 \psi_W(\omega) &= -2kx_W(\omega)\Lambda_W T_{iW} P_{LW}(\omega) (1 + R_{eW} P_{LW}(\omega) R_{iW} P_{LW}(\omega))^{-1} R_{eW} \psi_W^{ins}
 \end{aligned}$$

All operators with  $\omega$  argument can be obtained with the standard equations, just multiplying all propagators by the additional signal dephasing  $e^{i\omega L/c}$ .

## 7 List of symbols

$L_N, L_W$	arm cavity macroscopic lengths
$l_N, l_W$	short Michelson arm macroscopic length
$l_P, l_S$	power and signal recycling mirror distances from beam splitter
$l_{RC}, l_{SC}$	total power and signal recycling cavity lengths
$P_{LN}, P_{LW}$	arm propagators (matrices)
$P_{RC}, P_{SC}$	power and signal recycling cavity propagators (matrices)
$P_-$	short Michelson propagator (matrix)
$R_P, T_P$	reflection (as seen from inside ITF) and transmission operators for PR mirror
$R_S, T_S$	reflection (as seen from inside ITF) and transmission operators for SR mirror
$R_{iN}, T_{iN}$	reflection (as seen from inside arm) and transmission operators for north input mirror
$R_{eN}, T_{eN}$	reflection (as seen from inside arm) and transmission operators for north end mirror
$R_{iW}, T_{iW}$	reflection (as seen from inside arm) and transmission operators for west input mirror
$R_{eW}, T_{eW}$	reflection (as seen from inside arm) and transmission operators for west end mirror
$\Lambda_N, \Lambda_W$	input mirror lens operators for north and west arms
$F_N, F_W$	Fabry-Perot cavities reflection operators
$M_{AS}, M_{SA}, M_{SS}, M_{AA}$	Michelson interferometer operators between symmetric and anti-symmetric ports
$\omega$	signal frequency
$x_N, x_W$	microscopic displacements of end mirrors
$\delta l_N, \delta l_W$	microscopic static tuning of Fabry-Perot arm cavities (combinations of DARM and CARM)
$\delta l_{RC}$	microscopic static tuning of power recycling cavity (PRCL)
$\phi_{g,X}$	Gouy phase for $TEM_{00}$ in the X cavity
$\varphi_{SR}$	microscopic tuning of signal recycling cavity
$\psi_0$	interferometer input field
$\psi_{RC}$	static field inside power recycling cavity (at PR reflection inside PRC)
$\psi_{SC}$	static field inside signal recycling cavity (at BS reflection)
$\psi_{DF}$	static field at dark port
$\psi_N, \psi_W$	static fields at arm cavity input
$\psi_N^{ins}, \psi_W^{ins}$	static fields inside arm cavities

## References

- [1] Y. Pan, *Optimal degeneracy for the signal-recycling cavity in advanced LIGO*, arXiv:gr-qc/0608128 v1 (2006) [1](#)
- [2] Y. Hefetz, N. Mavalvala, D., Sigg, *Principles of calculating alignment signals in complex resonant optical interferometers*, LIGO-P960024-A-D (1996) [1](#)
- [3] A. E. Siegman, *Lasers*, University Science Book, Mill Valley California (1986) [2](#), [3](#)
- [4] J.Y. Vinet, *Virgo physics book*, [<http://www.casina.virgo.infn.it/vpb>] [3](#), [4](#)